INTERNATIONAL JOURNAL OF GEOGRAPHICAL INFORMATION SCIENCE
https://doi.org/10.1080/13658816.2019.1694681

Taylor & Francis
Taylor & Francis Group

RESEARCH ARTICLE

Empirical assessment of road network resilience in natural hazards using crowdsourced traffic data

Yi Qiang and Jinwen Xu

Department of Geography and Environment, University of Hawaii – Manoa, Honolulu, USA

ABSTRACT

Climate change and natural hazards pose great threats to road transport systems which are 'lifelines' of human society. However, there is generally a lack of empirical data and approaches for assessing resilience of road networks in real hazard events. This study introduces an empirical approach to evaluate road network resilience using crowdsourced traffic data in Google Maps. Based on the conceptualization of resilience and the Hansen accessibility index, resilience of road network is measured from accumulated accessibility reduction over time during a hazard. The utility of this approach is demonstrated in a case study of the Cleveland metropolitan area (Ohio) in Winter Storm Harper. The results reveal strong spatial variations of the disturbance and recovery rate of road network performance during the hazard. The major findings of the case study are: (1) longer distance travels have higher increasing ratios of travel time during the hazard; (2) communities with low accessibility at the normal condition have lower road network resilience; (3) spatial clusters of low resilience are identified, including communities with low socio-economic capacities. The introduced approach provides ground-truth validation for existing quantitative models and supports disaster management and transportation planning to reduce hazard impacts on road network.

ARTICLE HISTORY
Received 14 March 2019
Accepted 14 November 2019

KEYWORDS
Resilience; accessibility; crowdsourced data; empirical study; natural hazards; time-geography

1. Introduction

Road transport systems are 'lifeline' systems providing fundamental support for national security, economy, public welfare and individuals' daily activities. Disruptions of road transport systems can lead to significant socio-economic impacts. Due to the changing climate and increasing extreme weather events, much attention has been paid to the vulnerability and resilience of road transportation systems to the environmental stressors. Ample evidence shows that extreme weather events can cause significant disruptions to the performance of road networks (Koetse and Rietveld 2009), which affect people's accessibility to employment, shopping, health care, and emergency services. For example, a winter storm can cause billions of dollars' economic loss (National Oceanic and Atmospheric Administration (NOAA) 2018; Smith and Katz 2013), a large proportion of which is due to reduced performance of road networks (Fortune 2016). The impacts of hazards on road networks are various in space and time, depending on the physical

CONTACT Yi Qiang yi_qiang@hotmail.com

properties of road networks and a variety of environmental and socio-economic factors. It is of crucial importance to understand the complex interplay among the various factors and develop actionable metrics of road network resilience to guide planning, mitigation and emergency management.

Despite the available studies on measuring vulnerability and resilience of transport systems (will be reviewed in Section 2), there is a general lack of empirical methods for measuring resilience of road network in hazardous weather conditions. This issue is largely attributed to the challenge of collecting real-time and location-based traffic data using traditional means (e.g. traffic sensors or counters installed on roads). With the advent of Web 2.0, interactive web-map services (e.g. Google Maps® and Bing Maps®) are becoming platforms where numerous travelers acquire and share information at any time in any place. In addition to providing routing services to travelers, these crowd-sourced data create unique opportunities to monitor dynamic performance of road network in hazardous weather events and to obtain empirical knowledge about road network resilience.

This study introduces an innovative approach that utilizes mobility data crowdsourced in Google Maps® to analyze resilience of road network. Using travel times collected at a sequence of times during a weather event, dynamics of accessibility to critical facilities can be calculated for specific locations. Based on a conceptual framework of resilience, a novel approach is introduced to assess resilience of road network from accumulated accessibility reduction during the hazard. The utility of this approach is demonstrated in a case study of winter storm. The introduced approach fills the critical gap of empirical assessments for road network resilience in real hazard events. It helps to reveal the spatial variance of accessibility disturbance and the recovery rate of road networks during the hazards. The location-based resilience metric can provide actionable information for disaster management and transportation planning to mitigate hazard impacts on road transport systems.

The rest of the article is organized as follows: Section 2 presents a literature review of related studies and points out the current research gaps. Section 3 refines the conceptual framework of resilience and introduce the measurement method for road network resilience. Section 4 describes the process of data collection using Google Maps APIs and the settings in the case study of Cleveland, OH in Winter Storm Harper. Section 5 presents the analysis results in the case study. Section 6 discusses the implications, limitations and future directions.

2. Related work

As reviewed by Koetse and Rietveld (2009), abundant studies have been conducted to understand the impacts of hazardous weather conditions on road transport systems. Abundant evidence shows precipitation events can cause reduction of traffic speed in road networks. According to a report by Federal Highway Administration (1977), traffic speed reduces by 22% in a wet road condition and the reduction can reach to 42% in a snowy condition. The impact of weather on traffic speed has been confirmed in a series of subsequent studies (Ibrahim and Hall 1994, Martin *et al*. 2000, Hranac *et al*. 2006, Maze *et al*. 2006). Furthermore, Sabir *et al*. (2008) estimated that rain may cause € 0.88 welfare loss per commuting trip in the Netherlands due to increased travel time on road. In addition to traffic speed, precipitation events may also affect accident frequency (Edwards 1996, Eisenberg 2004, Chung *et al*. 2005) and severity (Khattak *et al*. 1998, Andrey *et al*. 2003, Eisenberg and Warner 2005), traffic volume (Hanbali and Kuemmel 1993, Knapp *et al*. 2000) and individuals' travel behaviors (Aaheim and Hauge 2005).

The concept of vulnerability was introduced to describe the susceptibility of road networks to incidents that can result in reduction in road network serviceability (Berdica 2002). Vulnerability of road networks is commonly measured by the reduction of accessibility due to hypothetical disruptions or failures in the network (e.g. Berdica and Eliasson 2004, Husdal 2004, Sohn 2006, Taylor *et al*. 2006, Chen *et al*. 2007). As the principal service provided by road transport systems, accessibility is defined as 'the potential of opportunities for interaction' (Hansen 1959) or 'the ease with which any land-use activity can be reached from a location using a particular transport system' (Dalvi and Martin 1976). Accessibility is a deep-seated concept in geography and urban planning, which plays a central role in studying the interactions among land use, transport systems and people (Kwan 2013, Neutens 2015). For vulnerability assessment, accessibility is often used as a proxy to estimate hazard impacts on transport serviceability and identify critical links the loss of which may lead to significant socio-economic consequences (Taylor and Susilawati 2012, Jenelius and Mattsson 2015).

Another related concept is resilience, which is sometimes considered the opposite of vulnerability. With an origin in ecological research, resilience expresses the capacity of systems to absorb disturbances and return to pre-disaster condition or a new equilibrium (Holling 1996, Adger *et al*. 2005). In the field of transportation, the definition of resilience includes the ability of resisting and absorbing disturbances (i.e. resistance) and the ability of adapting to disruptions, and returning to normal functionalities (i.e. recovery) (Faturechi and Miller-Hooks 2014a, Calvert and Snelder 2018). Resilience of road transport system is dependent on both the inherent capacity of the system in coping with disturbance and adaptive actions taken by humans that help the system to restore performance (Faturechi and Miller-Hooks 2014b). Despite the available studies of resilience in the broad area of transportation (e.g. Chen and Miller-Hooks 2011, Cox *et al*. 2011, Ishfaq 2012), quantitative assessment approaches for road network resilience are relatively rare. Noticeable contributions include the stochastic framework developed by Faturechi and Miller-Hooks (2014b), which can be used to quantify and optimize travel time resilience in roadway networks, and the Link Performance Index for Resilience by Calvert and Snelder (2018), which evaluates the resilience of individual road sections. Both of the frameworks are theory-driven, predicting resilience of road networks using mathematical models with presumed network properties and traffic conditions.

There are a few issues that have not been well addressed in current approaches for road network vulnerability and resilience. First, few empirical approaches are available for evaluating road network vulnerability or resilience in real disaster events. The existing approaches (e.g. Taylor *et al*. 2006, Miller-Hooks *et al*. 2012) are primarily based on simulation models, predicting the potential degradation of network performance in hypothetical hazardous conditions. However, the actual performance of road networks in real hazard events is dynamic and complex, dependent on not only physical network properties (e.g. topology, road type and capacity) (Hooper *et al*. 2013), but also environmental (e.g. weather and topography) (Pregnolato *et al*. 2017) and human factors (e.g. mitigation, emergency management and individuals' travel behavior) (Zheng and Ling

2013, Jacobsen *et al*. 2016). Empirical observations of road network performance are needed to validate the predictions of the theory-based models and unravel the complex interplays among the various factors. Second, most existing approaches provide a system-level assessment of the entire network (e.g. Cox *et al*. 2011) or sections of the network (Adams *et al*. 2011). Few studies provide location-specific metrics from a community's or individual's perspective. Resilience assessments at a fine spatial scale can provide more specific and actionable guidance for improving road network resilience and disaster management in different areas with diverse environmental and socio-economic conditions.

3. Measurement framework

According to the notion of resilience including resistance and recovery, resilience of road networks should be measured from both the reduction of performance due to disturbance and the speed of recovering to normal performance. Figure 1 illustrates four simplified scenarios of system performance during a hazard. Figure 1(a) can be ranked as low resilience due to both the large performance reduction (low resistance) and the slow recovery. In the other extreme, Figure 1(d) represent a high-resilience scenario where the system has a small performance reduction (high resistance) and fast recovery. However, the in-between situations are difficult to compare, as they are paired with either low resistance and faster recovery (e.g. Figure 1(b)) or high resistance and slow recovery (e.g. Figure 1(c)). The dynamics of road performance can be more complex than the scenarios in Figure 1 and include several reduction troughs or different recovery speeds at different phases. Such complex patterns cannot be measured by a simple combination of the maximum disturbance and average recovery speed.

In this study, the resilience of a road transport system is measured by the accumulated reduction of road network performance during a hazard process, which can be represented as the difference (gray area in Figure 1) between actual performance in the hazard and benchmark performance at the normal condition. The accumulated reduction is dependent on both the extent of performance reduction (indicating resistance) and the lasting time of the reduction (indicating recovery). Not only the extreme situations (e.g. Figure 1(a,d)), intermediate conditions (e.g. Figure 1(b,c)) and more complex patterns can be differentiated. Assuming road network performance during a hazard can be modelled as a function over time, resilience (R) can be calculated as the integral of the performance function $f(x)$ from the time when the performance decline below the normal condition

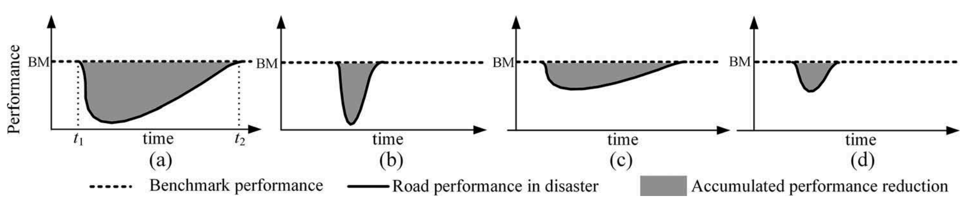

Figure 1. Possible scenarios of road network performance in a hazard. (a): a low-resilience scenario. (b-c): the intermediate resilience scenarios, (d): a high-resilience scenario.

(t_1) to the time when the accessibility restores to the normal condition (t_2) (see Equation 1).

$$R = \int_{t_1}^{t_2} f(x)dx \tag{1}$$

The Hansen accessibility index (Hansen 1959) is used as the indicator of road network performance. This index provides an overall measure of the accessibility from one location to a number of destinations. The original equation of the Hansen accessibility index can be written as:

$$A_i = \frac{\sum_j w_j f(c_{ij})}{\sum_j w_j} \tag{2}$$

where $f(c_{ij})$ is the ease from location i to destination j. $f(c_{ij})$ is negatively related with the travel cost (e.g. travel time) from i to j, which is denoted as c_{ij}. w_j is the attractiveness of destination j. In the introduced approach, travel cost c_{ij} is calculated as the reciprocal of travel time x_{ij} from location i to a nearby facility j . The attractiveness coefficients (w_j) is considered equal for all nearby facilities. Other weighting schemes can be applied when the relative importance among the facilities can be determined. Thus, the Hansen accessibility can be adapted as:

$$A_i = \frac{1}{n} \cdot \sum_{j=1}^{n} \frac{1}{x_{ij}} \tag{3}$$

where x_{ij} is the normalized travel time from Location i to Facility j. n is the number of nearby facilities of Location i. By comparing the actual Hansen index and benchmark Hansen index over time, the accumulated reduction of accessibility can be calculated as:

$$RA_i = \int_{t_1}^{t_2} \left(\frac{(A'_i(t) - A_i(t))}{A'_i(t)} \right) dt \tag{4}$$

where $A_i(t)$ and $A'_i(t)$ are the actual and benchmark Hansen index at Location i and Time t. RA_i is the accumulated reduction ratio of the Hansen index from t_1 to t_2. Road network resilience (R_i) is negatively proportional to the normalized value of RA_i, which is calculated as:

$$R_i = 1 - \frac{RA_i}{(max(RA) - min(RA))} \tag{5}$$

4. Data collection

The data collection includes the following steps. First, the nearby facilities of each location are acquired using the Search API of Google Maps. With the coordinates of a location and text keywords (e.g. 'hospital') in a request, the API returns 20 facilities near the search location, ranked by distance. n ($1 \le n \le 20$) of the 20 nearest facilities are selected to calculate accessibility. Next, in-traffic travel times from each location to the n nearest facilities at different times are acquired using the Direction API of Google Maps (Google 2019a). At a specific time (t), two travel times are retrieved for each location-facility pair with two different settings. The first travel time is requested with the departure time set to a future time corresponding to t. The retrieved travel time is an estimate based on the historical traffic condition at t on the same day of week. This travel time is considered as the benchmark reflecting the normal traffic condition. The second travel time is requested at exactly time t during the event, using 'now' as the departure time. This travel time indicates the actual traffic condition. Finally, travel times retrieved in the two settings are used to calculate the benchmark ($A_i'(t)$) and actual Hansen accessibility index ($A_i(t)$), respectively, at the time t. With requests at multiple time points during the disaster, the accumulated accessibility reduction (RA_i) is calculated using Equation 4, which is then used to calculate the resilience index (R_i) using Equation 5.

Data for the case study were collected in the metropolitan area of Cleveland, Ohio during Winter Storm Harper on January 19th and 20th, 2019, which was a major storm system that brought heavy snow from coast to coast in the United States. In the case study, in-traffic travel times from the centroid of each census tract to nearby facilities were requested at four time points, including 01/19/2019 11:00am (t_1), 01/19/2019 17:00pm (t_1) , 01/20/2019 11:00am (t_3), and 01/20/2019 17:00pm (t_4) Eastern Time. According to the weather record (National Oceanic and Atmospheric Administration (NOAA) 2019), t_1 was a time point before the storm impact arrived at Cleveland. Snow was the heaviest at t_2 and lasting until the midnight of the day. Snow fall stopped between t_2 and t_3. In addition, we defined 01/21/2019 0:00am (t_5), which is 22 h after the last hour with recorded snowfall, as the time point when the accessibility was no longer affected by the storm. We thus define the accessibility returns to the benchmark (i.e. reduction = 0) at t_5. An overall resilience score was calculated from the accumulated accessibility reduction from t_1 to t_5 for each census tract. In case the accessibility reduces later than t_1 or recovers to the benchmark earlier than t_5, only the negative part (i.e. the part below the benchmark) was counted in the calculation. Due to the small number of sampling times, linear interpolation was applied to estimate the accessibility reduction between the sampled time points. Other interpolation functions (e.g. polynomial functions) could be applied for a denser sampling frequency.

In the case study, the Hansen index was calculated using travel times to five types of facilities, including the center of the CBD, the nearest hospital, grocery store, police department and fire station. The CBD represents the concentration of employments, resources and services, which is often included in road accessibility and vulnerability assessments (Taylor *et al*. 2006, Taylor and Susilawati 2012). Grocery stores are places to obtain emergency supplies such as food, water, clothes and batteries for hazard preparation. Hospitals, police department and fire stations are critical facilities for emergency response (Federal Emergency Management Agency (FEMA) 2010). Locations of the nearby facilities around each tract were acquired using Google Search API. 41.505W and −81.686N was considered as the center of the CBD, which was returned from the Search API using 'Downtown, Cleveland, OH' as the keywords. The travel times were requested using the settings of 'fastest route' and 'driving mode'. The method can be expanded to other travel modes (e.g. transit, bike and walk) and other route criteria (e.g. the shortest route, avoid toll charge).

Selecting only five facility types and four sampling time points are primarily due to the cost of API usage. In the case study, the data collection includes 2,540 requests (635 census tract × 4 facility types excluding the CBD) to the Search API and 25,400 requests to the Direction API (635 census tract × 5 facility types × 4 time points × 2 settings). A request to the Search and Direction API costs $0.032 and $0.01, respectively (Google 2019b). The total requests result in a cost of $335.28 (2,540 × $0.032 + 25,400 × $0.01).

5. Analysis results

5.1. Travel time increase

Increases of travel time from census tracts to nearby facilities were identified during the winter storm. As illustrated in Figure 2, the average increasing ratio of travel times to the five types of facilities all peaked at t_2, when the snow fall was the heaviest. Particularly, the average travel time to the CBD increased by nearly 30% at t_2, while the average travel times to other facilities increased by less than 10%. Thus, t_2 can be considered the time when the disturbance of the overall network is maximum at the four sampled time points. At t_2, the increasing ratios of travel time are positively related to travel distances to most of the facilities (Figure 3), meaning that the storm impact is more severe for long-distance travels. The linear relations of the fire station, grocery store, police department, and hospital are all significant ($p < 0.05$) (Table 1). However, the increase ratio of travel times to the CBD shows a different pattern: the ratio increases until around 28 km and then starts to decline beyond this distance. This indicates that the storm impact to the accessibility to the CBD maximizes at a distance around 28 km. Whether this peak distance exists or varies in other cities and in other storms needs to be analyzed in future studies.

5.2. Accessibility reduction

The accessibility index at the pre-event time point (t_1) was slightly higher than the normal condition, possibly due to the higher traffic volume at t_1. To eliminate the bias of the different traffic volume, the benchmark accessibility at all the four times was adjusted by

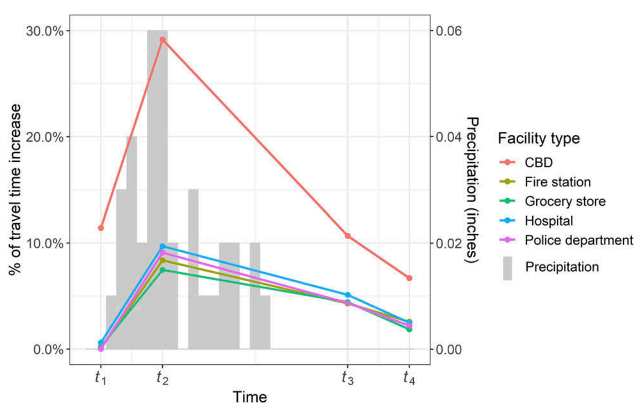

Figure 2. Average increasing ratios of travel time to the five types of facilities (refer to the left axis) and precipitation (refer to the right axis).

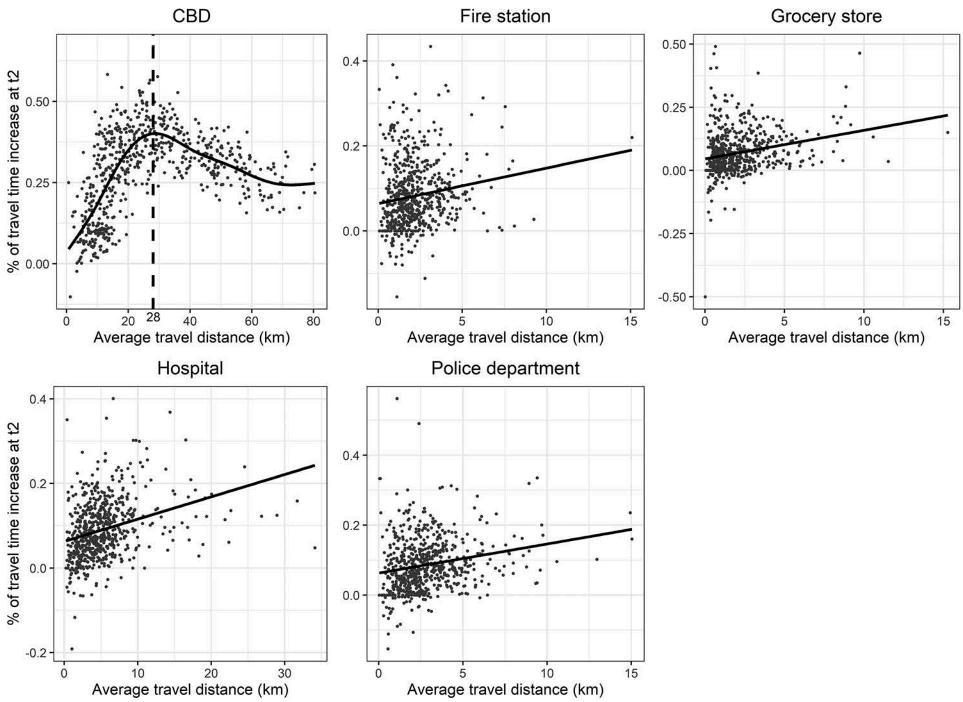

Figure 3. Relations between increasing ratios of travel time and travel distances. The relations of fire station, grocery stores, police department, and hospital are fitted in linear models. CBD is fitted in a generalized additive model. A summary of the regression models is reported in Table 1.

Table 1. Summary of the regression analyses. Scatter plots and regression lines can be found in Figures 3 and 8.

Dependent variable (y)	Independent variable (x)	Coefficient (β)	Residual (ε)	p	R^2	Degree of freedom
Ratio of travel time increase	Dist. to fire station	0.0061	0.0557	< 0.001	0.0292	635
	Dist. to grocery store	0.0082	0.0353	< 0.001	0.0586	635
	Dist. to hospital	0.0046	0.0468	< 0.001	0.0948	635
	Dist. to police department	0.0069	0.0480	< 0.001	0.0593	635
Normal accessibility	Accessibility reduction at t_2	1.5785	0.7711	< 0.001	0.3263	635
Normal accessibility	Resilience	0.3417	0.3925	< 0.001	0.1334	635
Accessibility reduction at t_2	Mean income	−2.25e-07	−0.0403	< 0.001	0.0578	632
Resilience	Mean income	−2.49e-07	0.8682	< 0.001	0.0082	632

the difference between the actual and benchmark accessibility at t_1, so that the accessibility reduction at t_1 became zero. The average accessibility reduction of the census tracts at different time points are illustrated in Figure 4(a), showing that the accessibility had the highest reduction at t_2 and gradually restored towards the benchmark at t_3 and t_4. The accessibility reduction differs at different census tracts at different times (Figure 4(b)). Spatially speaking, census tracts near the CBD and along the east part of lake shore had less accessibility reduction at t_2 (Figure 5). However, at t_3 and t_4, the distant census tracts recovered more quickly than the census tracts near the CBD. The spatial variance of accessibility reduction can be potentially explained by the physical conditions (network

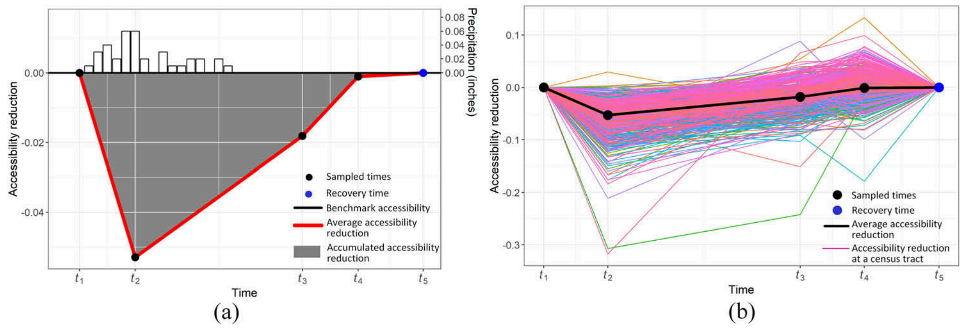

Figure 4. Average accessibility reduction at different times during the storm. (a) The average reduction of all census tracts. (b) The reduction at different census tracts.

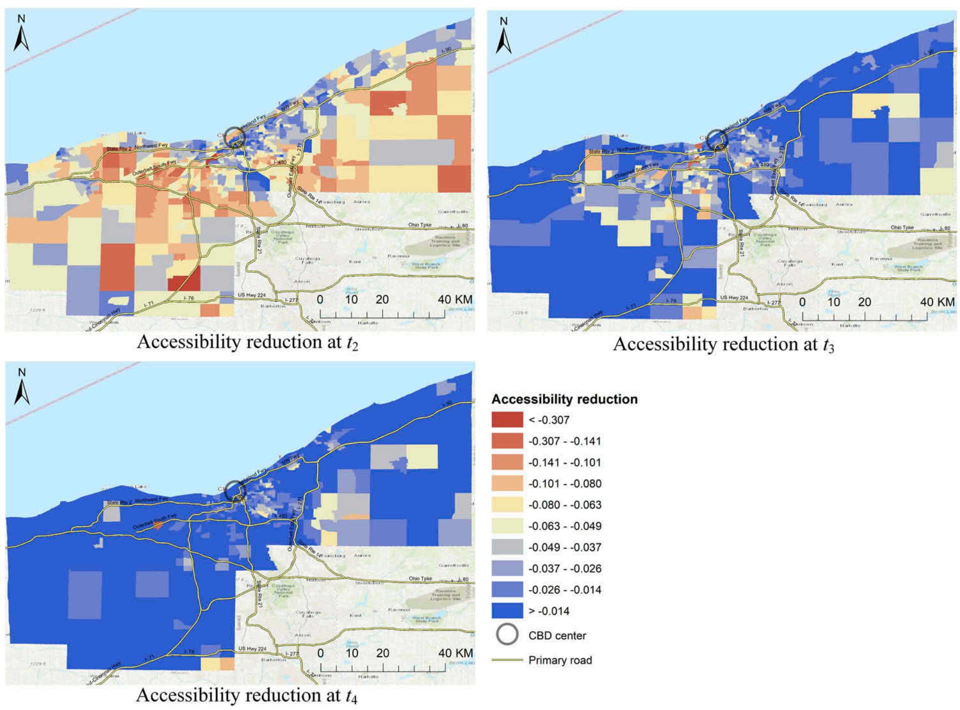

Figure 5. Spatial distribution of accessibility reduction in census tracts at *t*2, *t*3, and *t*4.

topology, road type and capacity) as well as human interventions (e.g. snowplow and adapted travel behaviors).

5.3. Resilience

As shown in Figure 6, the spatial distribution of overall resilience scores is uneven. Census tracts with a low-resilience score are colored in red to express an alarming signal in these places. In general, census tracts with a high-resilience score are mostly distributed along the lakeshore north in parallel with the I-90 interstate highway. Low-resilience scores are

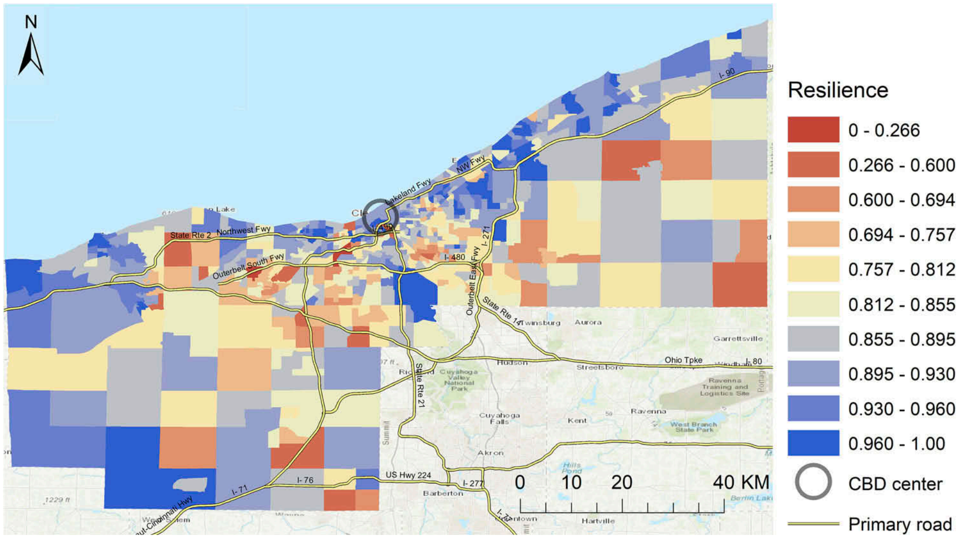

Figure 6. Spatial distribution of road network resilience in census tracts.

scattered in the inland area to the south of the lakeshore. The Getis-Ord Gi* analysis (Getis and Ord 1992) was applied to detect local clusters of resilience that are statistically significant at different probability levels (see Figure 7). A high-resilience cluster (also called 'hot spot') refers to a contiguous area where high-resilience census tracts are located near each other, while a low-resilience cluster (cold spot) represents the opposite. The result of the Getis-Ord Gi* analysis (Figure 7) further confirms the visual observation in Figure 6: most of the high-resilience clusters are located along the I-90 highway near the lakeshore.

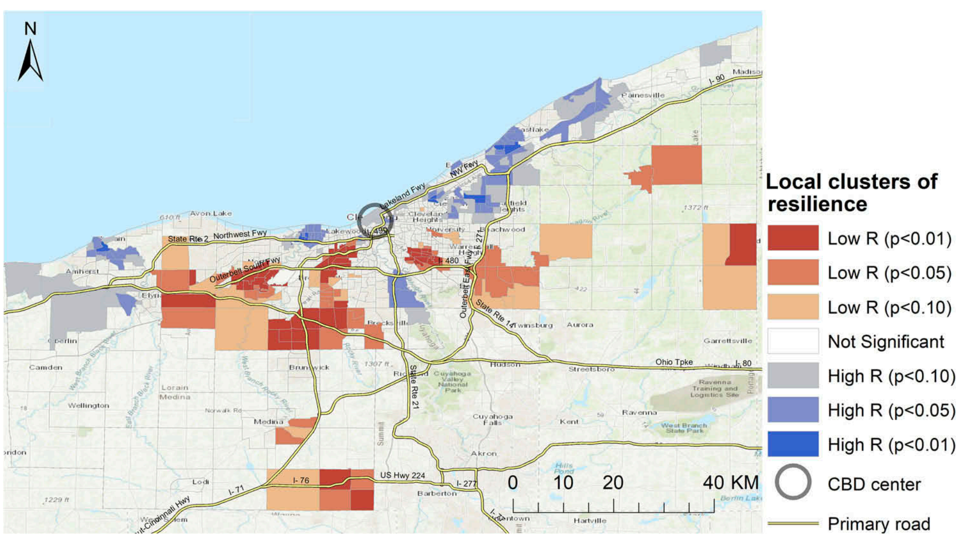

Figure 7. Hotspot analysis of road network resilience in census tracts.

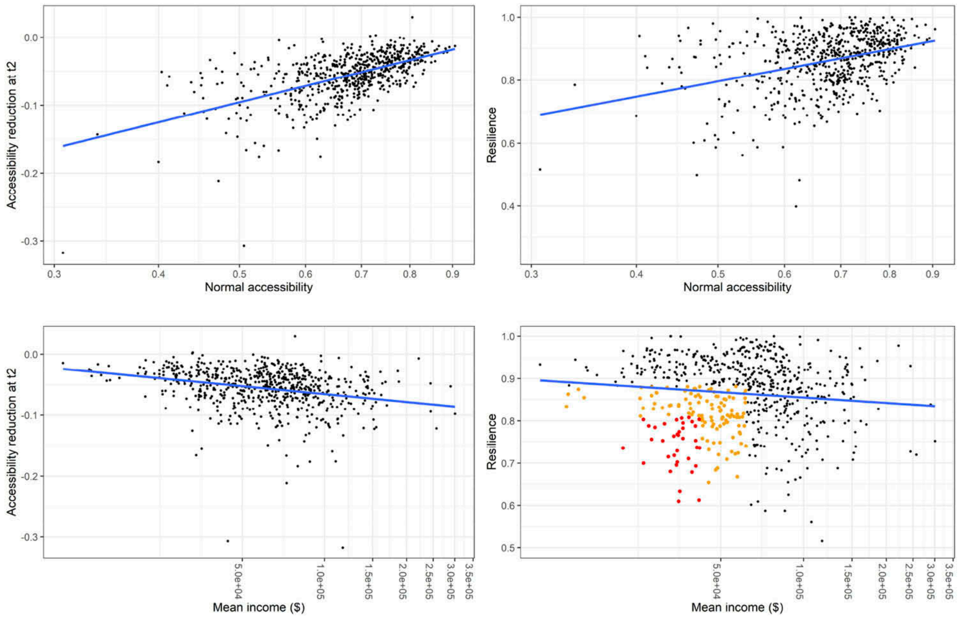

Figure 8. Relations between normal accessibility and accessibility reduction at *t*2. (b): The relation between normal accessibility and resilience. (c): The relation between mean income and accessibility reduction at *t*2. (d): The relation between income and resilience of road network. Blue lines are the regression lines. Orange and red points in (d) are census tracts where the mean income and resilience are both in the lower 50% quantile and 25% quantile, respectively.

5.4. Relations between variables

As shown in Figure 8(a,b), the accessibility reduction at t_2 (the time point of the maximum reduction) and the overall resilience are both positively related with the normal accessibility. These results indicate that census tracts that have longer travel times to the facilities at the normal condition experienced a higher level of disturbance and/or slower recovery in the storm. These results also confirm the analyses in Figure 3 where longer distance travels are associated with higher increases in travel time to the facilities. The accessibility reductions at t_2 (maximum disturbance) and resilience are negatively related with mean incomes (Figure 8(c,d)), indicating that the higher-income communities were more affected in the storm. These relations can be attribute to the demographic landscape in Cleveland: the low-income communities tend to be located near the CBD where the density of the selected facilities is high and so as the accessibility. Note, this study uses travel time by driving to measure accessibility, which assumes equal access to a vehicle. Future studies should consider the inequalities in vehicle ownership and access to other transportation systems (e.g. transit). Still, some low-income communities with low resilience of road network are noticeable. Figure 9 highlights the census tracts where the income and road network resilience are both at the lower quantiles (25% and 50%). As one of the most important indicator of social vulnerability and resilience (Cutter *et al*. 2003, 2010, Lam *et al*. 2015, Cai *et al*. 2018), income is often related with the capacity of communities and individuals to cope with and adapt to the adverse impacts of hazards.

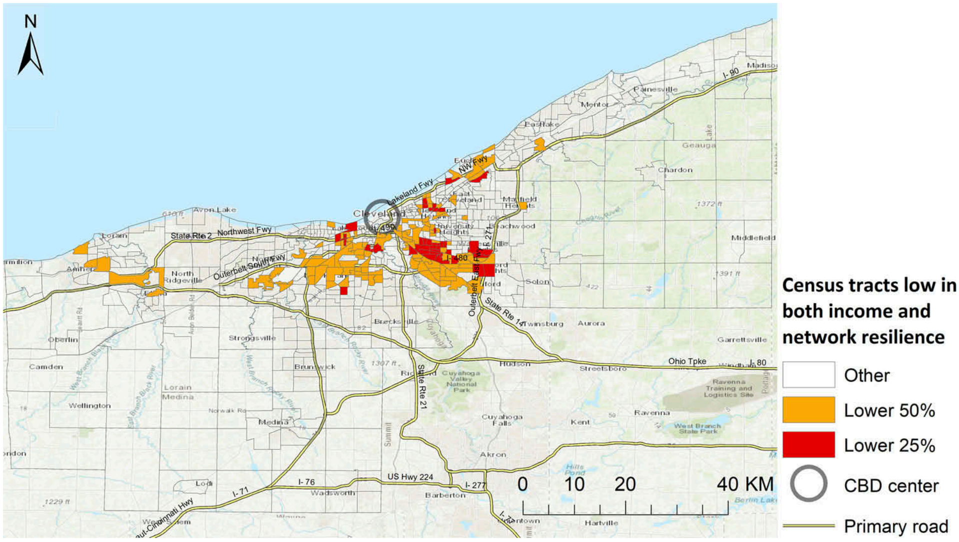

Figure 9. Census tracts where the mean income and resilience are both in the lower 50% quantile and 25% quantile. Colors of the tracts correspond to the colored points in Figure 8 (b).

Given the low resilience of road network and socio-economic capacities, more attention should be paid to these communities to minimize the adverse impacts of the storm.

6. Discussion

The study demonstrates the utility of the crowdsourced mobility data from Web 2.0 platforms for assessment of road network resilience. The introduced approach measures resilience of road networks using ground-truth data collected in real-disaster events. Other than Google Maps, the measurement approach is applicable to similar data services provided by Microsoft Bing Maps, ArcGIS for Developers, and Uber Movement. Compared with traditional data collection methods (e.g. installation of road sensors and field data collection), the crowdsourced data can be acquired at real-time and at a relatively low cost. Despite the simple settings (e.g. only the nearest facility and five time points) applied in the case study, the introduced assessment approach can be easily expanded to a larger region, a longer period, more facilities, and/or a higher sampling frequency (e.g. hourly sampling). Not limited to winter storms, the approach can be applied in other hazards such as hurricane, king tide, sea level rise, and land slide that may cause accessibility reduction in road networks. With applications in more hazard events and larger geographical areas, this approach can increase the knowledge about the complex factors of road network resilience. Such knowledge is generally lacking but crucial for building resilient and sustainable transportation systems. Additionally, this approach can be implemented in an interactive interface for emergency responders to monitor real-time accessibility at different locations and identify communities in urgent need for assistance and disaster relief.

The effectiveness of hazard mitigation and emergency management can be evaluated by comparing assessments in different case studies. Using the same approach, the preliminary results shows a more complex pattern of network performance in Seattle in

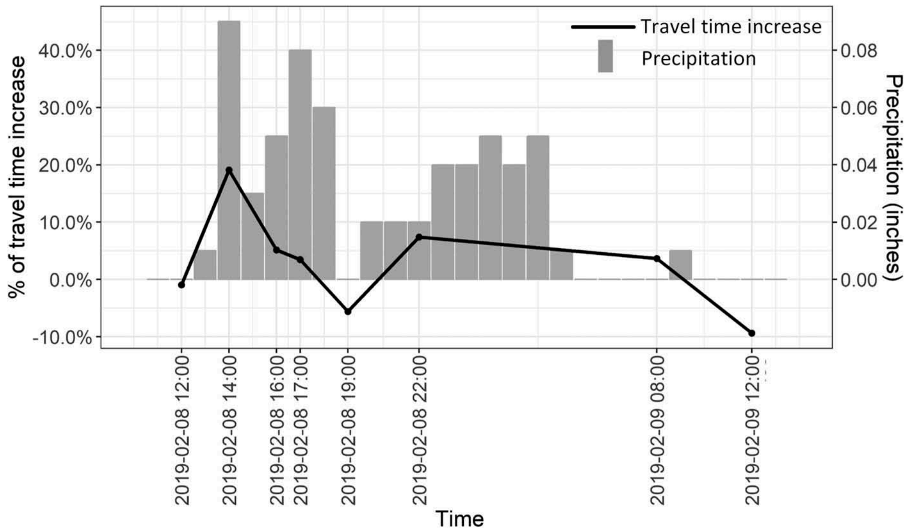

Figure 10. Average increase ratio of travel time from the CBD to census tracts in the Seattle metropolitan area during Winter Storm Maya.

Winter Storm Maya (see Figure 10): the average increase of travel times to the CBD peaked for a short period at the very beginning of the storm (at around 14:00pm on Friday, 02/08/2019), and then quickly declined and stayed at a lower level afterwards. In the normal rush hour on Fridays (16:00–17:00 according to TomTom 2016), the travel time has returned near the normal condition, although the snowfall continued. The short disturbance period may be attributed to the effective emergency response in Seattle, including the timely issuance of winter storm warnings and the early release of schools at noon on the day. In addition to the case-by-case findings, general lessons about effective mitigation and emergency management can be gained from applications of this approach in more hazard events and larger geographical areas.

The case study is limited to the measurement of accessibility to a few selected facilities. A complete assessment of road network resilience should consider the disturbance of individuals' maximum mobility in space and time. As a profound conceptual model in time-geography, the space-time prism (Hägerstraand 1970) represents individuals' maximum travel extents or interaction potential in space and time as 3D prisms (Miller 2005, Neutens *et al*. 2008). A future extension of the introduced approach could be the integration with space-time prisms. The resilience of road network for an individual person can be measured from the accumulated shrink of a 3D prism which represents his maximum mobility in space and time. Such location- or individual-level assessments of road network resilience can support real-time decision-making in hazard events and improve humanized transportation planning. Example questions can be answered include: which communities are experiencing the greatest accessibility reduction during a hazard? Are the socially vulnerable communities located in areas with low network resilience? Are there communities or population groups systematically or disproportionally affected due to low resilience of road networks?

7. Conclusion

This study introduces an empirical approach to assess road network resilience using crowd-sourced traffic data from Google Maps. Built on the conceptualization of resilience and the Hansen accessibility index, accumulated accessibility reduction over time is used to measure resilience of road network during natural hazards. The utility of this approach is demonstrated in a case study of the Cleveland metropolitan area (Ohio) in Winter Storm Harper. The results reveal strong spatial variations of the disturbance and recovery rate of road network performance during the hazard event. The findings in the case study are: (1) longer distance travels have higher increasing ratios of travel time during the hazard; (2) communities with low accessibility at the normal condition have lower resilience (great and long-lasting accessibility reduction) in the local road networks; (3) the spatial clusters of low network resilience are identified. The study also suggests that special assistance should be applied to the communities where both road network resilience and socio-economic capacities (e.g. low income) are lower than the average. Utilizing crowdsourced geospatial data, this study filled the void of empirical assessment of road network resilience at real-time and real-place. The assessment results can provide ground-truth validation for existing quantitative models to better predict road network resilience in extreme weather events. Integrated with the theoretical frameworks of time-geography, this approach can be further expanded to model the dynamic aspects of road network resilience and advance research about the social issues (i.e. environmental justice and social equalities) related to transportation planning.

Disclosure statement

No potential conflict of interest was reported by the authors.

Notes on contributors

Yi Qiang is an Assistant Professor in the Department of Geography and Environment at the University of Hawai'i at Manoa. He holds a Ph.D. in Geography from Ghent University, Belgium. His research areas include in space-time modeling, visual analytics, geocomputation, disaster risk assessment, dynamic modeling of coupled natural and human (CNH) systems.

Jinwen Xu is a Ph.D. student in the Department of Geography and Environment, University of Hawaii at Manoa. He holds a master degree in Urban and Environmental Planning from Arizona State University. He is interested in Geographical Information Science, spatial analysis, social media big data, and natural disaster.

Data and codes availability statement

The data and codes that support the findings of this study are available in figshare.com with the identifier(s) [doi.10.6084/m9.figshare.10279295.v1].

Funding

This article is based on work supported by two research grants from the U.S. National Science Foundation: one under the Coastlines and People (CoPe) Program (Award No. 1940091) and the other under the Methodology, Measurement & Statistics (MMS) Program (Award No. 1853866). Any opinions, findings, and conclusions or recommendations expressed in this material are those of the authors and do not necessarily reflect the views of the funding agencies.

ORCID

Yi Qiang http://orcid.org/0000-0002-6872-8837

References

Aaheim, H.A. and Hauge, K.E., 2005. Impacts of climate change on travel habits: a national assessment based on individual choices. Available from: https://pub.cicero.oslo.no/cicero-xmlui/handle/11250/191992

Adams, T., Bekkem, K.R., and Bier, V.M., 2011. Evaluating freight transportation resilience on a highway corridor. In: Transportation Research Board (90th Annual Meeting of Transportation Research Board, 2011). Available from: https://trid.trb.org/view/1093083 [Accessed 23 Aug 2019]

Adger, W.N., *et al*., 2005. Social-ecological resilience to coastal disasters. *Science*, 309, 1036–1039. doi:10.1126/science.1112122

Andrey, J., *et al*., 2003. Weather as a chronic hazard for road transportation in Canadian cities. *Natural Hazards Research*, 28, 319–343. doi:10.1023/A:1022934225431

Berdica, K., 2002. An introduction to road vulnerability: what has been done, is done and should be done. *Transportation Policy*, 9, 117–127. doi:10.1016/S0967-070X(02)00011-2

Berdica, K. and Eliasson, J., 2004. Regional accessibility analysis from a vulnerability perspective. Presented at the the second international symposium on transportation network reliability. INSTR. http://urn.kb.se/resolve?urn=urn:nbn:se:kth:diva-77205

Cai, H., *et al*., 2018. A synthesis of disaster resilience measurement methods and indices. *International Journal of Disaster Risk Reduction : IJDRR*. doi:10.1016/j.ijdrr.2018.07.015

Calvert, S.C. and Snelder, M., 2018. A methodology for road traffic resilience analysis and review of related concepts. *ACS Pharmacology & Translational Science*, 14, 130–154.

Chen, A., *et al*., 2007. Network-based accessibility measures for vulnerability analysis of degradable transportation networks. *Networks and Spatial Economics (NETW SPAT ECON)*, 7, 241–256. doi:10.1007/s11067-006-9012-5

Chen, L. and Miller-Hooks, E., 2011. Resilience: an indicator of recovery capability in intermodal freight transport. *Transportation Science*, 46, 109–123. doi:10.1287/trsc.1110.0376

Chung, E., *et al*., 2005. Effect of rain on travel demand and traffic accidents, In: Proceedings. 2005 IEEE intelligent transportation systems, 2005. 1080–1083. doi:10.1109/ITSC.2005.1520201

Cox, A., Prager, F., and Rose, A., 2011. Transportation security and the role of resilience: A foundation for operational metrics. *Transportation Policy*, 18, 307–317. doi:10.1016/j.tranpol.2010.09.004

Cutter, S.L., Boruff, B.J., and Shirley, W.L., 2003. Social vulnerability to environmental hazards. *Social Science Japan Journal*, 84, 242–261. doi:10.1111/1540-6237.8402002

Cutter, S.L., Burton, C.G., and Emrich, C.T., 2010. Disaster resilience indicators for benchmarking baseline conditions. *Journal of Homeland Security and Emergency Management*, 7, 14.

Dalvi, M.Q. and Martin, K.M., 1976. The measurement of accessibility: some preliminary results. *Transportation*, 5 (1), 17–42. doi:10.1007/BF00165245

Edwards, J.B., 1996. Weather-related road accidents in England and Wales: a spatial analysis. *Journal of Transport Geography*, 4, 201–212. doi:10.1016/0966-6923(96)00006-3

Eisenberg, D., 2004. The mixed effects of precipitation on traffic crashes. *Accident; Analysis and Prevention*, 36, 637–647. doi:10.1016/S0001-4575(03)00085-X

Eisenberg, D. and Warner, K.E., 2005. Effects of snowfalls on motor vehicle collisions, injuries, and fatalities. *American Journal Public Health*, 95, 120–124. doi:10.2105/AJPH.2004.048926

Faturechi, R. and Miller-Hooks, E., 2014a. Measuring the performance of transportation infrastructure systems in disasters: A comprehensive review. *Journal of Infrastructure Systems*, 21, 04014025. doi:10.1061/(ASCE)IS.1943-555X.0000212

Faturechi, R. and Miller-Hooks, E., 2014b. Travel time resilience of roadway networks under disaster. *Transportation Research Part B: Methodological*, 70, 47–64. doi:10.1016/j.trb.2014.08.007

Federal Emergency Management Agency (FEMA), 2010. Developing and maintaining emergency operations plans, Comprehensive Preparedness Guide (CPG) 101. Available from: https://www.fema.gov/media-library/assets/documents/25975

Federal Highway Administration. 1977. Economic impact of highway snow and ice control, final report (No. FHWA-RD-77-95). https://rosap.ntl.bts.gov/view/dot/30611/dot_30611_DS1.pdf

Fortune, 2016. Here's how much Winter Storm Jonas Cost the East Coast. http://fortune.com/2016/01/25/winter-storm-jonas-economic-impact/

Getis, A. and Ord, J.K., 1992. The analysis of spatial association by use of distance statistics. *Geographical Analysis*, 24, 189–206. doi:10.1111/j.1538-4632.1992.tb00261.x

Google, 2019a. Maps JavaScript API - directions service. https://developers.google.com/maps/documentation/javascript/directions

Google, 2019b. Maps JavaScript API usage and billing. https://developers.google.com/maps/documentation/javascript/usage-and-billing

Hägerstraand, T., 1970. What about people in regional science? *Papers in Regional Science : the Journal of the Regional Science*. doi:10.1111/j.1435-5597.1970.tb01464.x

Hanbali, R.M. and Kuemmel, D.A., 1993. Traffic volume reductions due to winter storm conditions, in: transportation research record. Presented at the third international symposium on snow removal and ice control technology, Minneapolis, Minnesota.

Hansen, W.G., 1959. How accessibility shapes land use. *Journal of the American Planning Association*, 25, 73–76. doi:10.1080/01944365908978307

Holling, C.S., 1996. Engineering resilience versus ecological resilience. *Engineering Within Ecological Constraints*, 31, 32.

Hooper, E., Chapman, L., and Quinn, A., 2013. The impact of precipitation on speed–flow relationships along a UK motorway corridor. *Theoretical and Applied Climatology*, 117 (1), 303–316. doi:10.1007/s00704-013-0999-5

Hranac, R., *et al*., 2006. Empirical studies on traffic flow in inclement weather (No. publication No. FHWA-HOP-07-073). Washington, DC: Federal Highway Administration. Available from: https://vtechworks.lib.vt.edu/handle/10919/55110

Husdal, J., 2004. Reliability and vulnerability versus cost and benefits, In: Proc. 2nd Int. Symp. Transportation Network Reliability (INSTR), Christchurch, New Zealand. 180–186.

Ibrahim, A.T. and Hall, F.L., 1994. Effect of adverse weather conditions on speed-flow-occupancy relationships. *Transportation Research Record*.

Ishfaq, R., 2012. Resilience through flexibility in transportation operations. *International Journal of Logistics Research and Applications*, 15, 215–229. doi:10.1080/13675567.2012.709835

Jacobsen, J.K.S., Leiren, M.D., and Saarinen, J., 2016. Natural hazard experiences and adaptations: A study of winter climate-induced road closures in Norway. *Norsk Geografisk Tidsskrift - Norwegian Journal of Geography*, 70 (5), 292–305. doi:10.1080/00291951.2016.1238847

Jenelius, E. and Mattsson, L.-G., 2015. Road network vulnerability analysis: conceptualization, implementation and application. *Computers, Environment and Urban Systems*, 49, 136–147. doi:10.1016/j.compenvurbsys.2014.02.003

Khattak, A.J., Kantor, P., and Forrest, C., 1998. Role of adverse weather in key crash types on limited-access: roadways implications for advanced weather systems | request PDF. *Transportation Research Record Journal of the Transportation*, 1621, 10–19. doi:10.3141/1621-02

Knapp, K., Kroeger, D., and Giese, K., 2000. Mobility and safety impacts of winter storm events in a freeway environment. Iowa DOT project TR-426; CTRE management project 98-39. Iowa State University. Center for Transportation Research and Education. https://rosap.ntl.bts.gov/view/dot/23579

Koetse, M.J. and Rietveld, P., 2009. The impact of climate change and weather on transport: an overview of empirical findings. *Transportation Research. Part D, Transport and Environment*, 14, 205–221. doi:10.1016/j.trd.2008.12.004

Kwan, M.-P., 2013. Beyond space (as we knew it): toward temporally integrated geographies of segregation, health, and accessibility. *Annals of the Association of American Geographers*, 103 (5), 1078–1086. doi:10.1080/00045608.2013.792177

Lam, -N.S.-N., *et al*., 2015. Mapping and assessing coastal resilience in the Caribbean region. *Cartography and Geographic Information Science*, 0406, 1–8. doi:10.1080/15230406.2015.1040999

Martin, P.T., *et al*., 2000. Inclement weather signal timings (No. UTL Research Report MPC01-120). Salt Lake City: Utah Traffic Lab, University of Utah.

Maze, T.H., Agarwal, M., and Burchett, G., 2006. Whether weather matters to traffic demand, traffic safety, and traffic operations and flow. *Transportation Research Record: Journal of the Transportation Research Board 1948*. doi:10.1177/0361198106194800119

Miller, H.J., 2005. A measurement theory for time geography. *Geographical Analysis*, 37, 17–45. doi:10.1111/j.1538-4632.2005.00575.x

Miller-Hooks, E., Zhang, X., and Faturechi, R., 2012. Measuring and maximizing resilience of freight transportation networks. *Computers & Operations Research*, 39 (7), 1633–1643. doi:10.1016/j.cor.2011.09.017

National Oceanic and Atmospheric Administration (NOAA), 2018. U.S. Billion-Dollar Weather & Climate Disasters 1980-2018. Available from: https://www.ncdc.noaa.gov/billions/events.pdf

National Oceanic and Atmospheric Administration (NOAA) 2019. U.S. Hourly Precipitation Data. https://data.nodc.noaa.gov/cgi-bin/iso?id=gov.noaa.ncdc:C00313

Neutens, T., 2015. Accessibility, equity and health care: review and research directions for transport geographers. *Journal of Transport Geography*, 43, 14–27. doi:10.1016/j.jtrangeo.2014.12.006

Neutens, T., *et al*., 2008. A three-dimensional network-based space–time prism. *Journal of Geographical Systems*, 10, 89–107. doi:10.1007/s10109-007-0057-x

Pregnolato, M., *et al*., 2017. The impact of flooding on road transport: A depth-disruption function. *Transportation Research Part D: Transport and Environment*, 55, 67–81. doi:10.1016/j.trd.2017.06.020

Sabir, M., *et al*., 2008. Welfare effects of adverse weather through speed changes in car commuting trips (SSRN Scholarly Paper No. ID 1269333). Rochester, NY: Social Science Research Network. Available from: https://papers.ssrn.com/abstract=1269333

Smith, A.B. and Katz, R.W., 2013. US billion-dollar weather and climate disasters: data sources, trends, accuracy and biases. *Natural Hazards Research*, 67, 387–410. doi:10.1007/s11069-013-0566-5

Sohn, J., 2006. Evaluating the significance of highway network links under the flood damage: an accessibility approach. *Transportation Research. Part A, Policy and Practice*, 40, 491–506. doi:10.1016/j.tra.2005.08.006

Taylor, M.A.P., Sekhar, S.V.C., and D'Este, G.M., 2006. Application of accessibility based methods for vulnerability analysis of strategic road networks. *Networks and Spatial Economics (NETW SPAT ECON)*, 6, 267–291. doi:10.1007/s11067-006-9284-9

Taylor, M.A.P. and Susilawati., 2012. Remoteness and accessibility in the vulnerability analysis of regional road networks. Network vulnerability in large-scale transport networks. *Transportation Research. Part A, Policy and Practice*, 46, 761–771. doi:10.1016/j.tra.2012.02.008

TomTom, 2016. TomTom traffic index. Available from: https://www.tomtom.com/en_gb/trafficindex/city/seattle

Zheng, Y.J. and Ling, H.F., 2013. Emergency transportation planning in disaster relief supply chain management: a cooperative fuzzy optimization approach. *Soft Computing*, 17 (7), 1301–1314. doi:10.1007/s00500-012-0968-4